Journal of Applied Polymer Science

Preparation and application of aluminum-doped zinc oxide powders via precipitation and plasma processing method

Xianjun Wang,[1] Ping Zhang,[2] Ruoyu Hong[1,2]

[1]School of Chemical Engineering, Fuzhou University, Fuzhou 350108, China

[2]College of Chemistry, Chemical Engineering and Materials Science & Key Laboratory of Organic Synthesis of Jiangsu Province, Soochow University, SIP, Suzhou 215123, China

Correspondence to: R. Y. Hong (E-mail: rhong@suda.edu.cn)

ABSTRACT: Aluminum-doped zinc oxide (AZO) conductive powders were successfully obtained through an attractive method based on the pyrolysis of coprecipitated precursors in arc plasma processing. The as-prepared powders were characterized by the x-ray diffraction (XRD), transmission electron microscopy (TEM), and UV-vis spectrum. The results reveal that Al atoms are doped into ZnO lattice successfully and all the samples are polycrystalline with a hexagonal wurtzite structure. Moreover, the particle size of aluminum doped zinc oxide prepared from the plasma pyrolysis was smaller than conventional thermal calcination. Afterward, the synthesized powders were reinforced into polypropylene (PP) matrix and the dispersion of the AZO filler in the PP matrix was observed by SEM. In addition, the effect of AZO concentrations on the electrical and mechanical properties of PP composites was investigated via resistance measurement, tensile and impact tests, respectively. The results show that the electrical and mechanical properties depend on the concentration and dispersion of AZO nanoparticles in the matrix. © 2015 Wiley Periodicals, Inc. J. Appl. Polym. Sci. **2015**, *132*, 41990.

KEYWORDS: composites; conducting polymers; mechanical properties; properties and characterization; thermal properties

Received 7 September 2014; accepted 17 January 2015

DOI: 10.1002/app.41990

INTRODUCTION

In modern industrial society, nanocomposites have become incredibly important in various fields, such as semiconductor devices, optoelectronic devices, textiles, medicine, cosmetics, agriculture, food packing, construction, and so on.[1–5] Nanocomposites are usually prepared by introducing inorganic nanoparticles into organic polymer matrix, which offers an effective way to improve the physical properties of pure polymers such as electrical, mechanical, antibacterial, thermal, catalytic, and optical properties.[6–11] In addition, the enhancement of nanocomposites properties mainly depends on the type, dispersion, contents, size, morphology of inorganic nanoparticle, and so on.[12–14]

Among the most versatile polymer matrices, polyolefine, such as polypropylene (PP), is one of the most widely used and fastest growing thermoplastics. PP continues to be an important engineering polymer because of its well-balanced physical and mechanical properties and their easy processability at a relatively low cost. Physical and mechanical properties of PP are generally modified by melt mixing with other polymers[15] and addition of small particle size filler, such as clay minerals consisting of silicate layers, silica, carbon nanotubes (CNTs), ZnO, TiO_2, and so on.

Zinc oxide (ZnO) has antioxidation, high temperature resistance, and good chemical stability. The ZnO powders are a class of material with important applications in optoelectronic device, sensor, energy material, transparent conducting electrodes, and other fields.[16] For many of these applications, the electrical conductivity and optical transmissivity are of key importance. Thus, the doped ZnO has attracted much attention for its low resistivity and high optical transmissivity in the visible range and good substrate adherence. The most common dopants for ZnO are group III elements such as boron (B),[17] aluminum (Al),[18] gallium (Ga),[19] and indium (In).[20] Among these materials, the Al-doped ZnO (AZO) is the most popular conductive material because of its high optical transparency, light color, high sensitivity, and increasing the ZnO conductivity without impairing the optical transmission, so it is regarded as a potential alternative candidate for ITO materials.[21]

Several methods have been used for the preparation of AZO, such as solvothermal method,[22] sol–gel method,[23] thermal evaporation method,[24] vapor deposition method,[25] pulsed laser deposition method,[26] magnetron sputtering method,[27] and coprecipitation method.[28] In particular, the co-precipitation method has the advantage of simple and low cost and has been

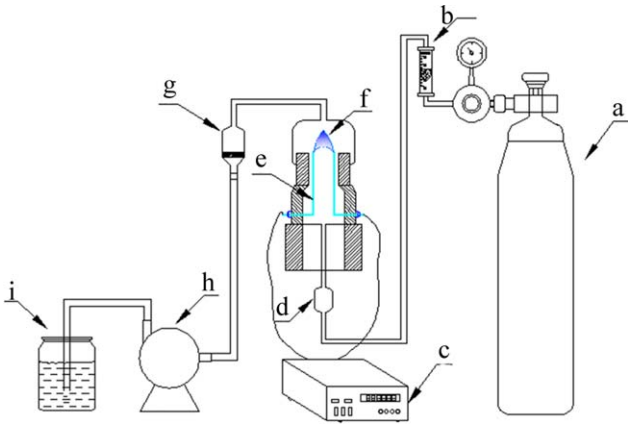

Figure 1. The experimental setup of plasma processing for the preparation of AZO powders. (a) Argon gas cylinders; (b) flowmeter; (c) Power supply; (d) Feed tank; (e) Copper electrode; (f) Plasma arc; (g) Sand core funnel; (h) Air pump; (i) Gas washing bottle. [Color figure can be viewed in the online issue, which is available at wileyonlinelibrary.com.]

used widely. According to the literature,[29] the coprecipitated precursors which were pre-calcined at 400°C for 2 h and then post-calcined at 900°C for 2 h in reducing atmosphere could show the low resistivity. However, the as-prepared powders have low optical transmissivity, and this method needs high temperature and long time.

Plasma processing is a simple method with characteristics of short sintering time, rapid temperature rise and uniform heating for sintered bodies, and has been applied in the preparation of functional materials, ceramics, intermetallic compounds, and so on.[30–32] Therefore, plasma processing can be an ideal technique to replace the traditional high temperature calcination. Moreover, plasma technology as an unconventional means has shown broad application prospects in improving the nanoscale powders dispersion, synthesis of ultrafine particles.[33] The size of such nanoparticles was reported to be 10–70 nm at relatively low powder feed rates.[34,35]

In this article, aluminum-doped zinc oxide powders of high performance could be prepared with the assist of arc plasma technology. The effects of plasma treatment on the structure, morphology, and optical property of the AZO particles were investigated. In addition, the as-prepared AZO powders were incorporated into the polypropylene (PP) to form inorganic–organic composites. The effects of incorporating AZO powders into the polypropylene (PP) matrix on electrical property, mechanical property, and thermostability were investigated.

EXPERIMENTAL

Materials

Zinc chloride ($ZnCl_2$), aluminum nitrate (Al $(NO)_3{\cdot}9H_2O$), sodium hydroxide (NaOH), anhydrous sodium carbonate (Na_2CO_3), polyethylene glycol 1000 (PEG-1000), and polypropylene (PP) were all of analytical grade and purchased from Wuxi Chemical Co. Two rods (4 mm in diameter) were used as the anode and cathode. Deionized water was used throughout the experiments.

Precursor Preparation

A simple chemical co-precipitation method was applied for the synthesis of the AZO precursor. The preparation process described as follows: $ZnCl_2$ and Al $(NO)_3{\cdot}9H_2O$ with the molar ratio of n (Al)/n (Zn) = 1.5 at % were firstly dissolved in deionized water, and PEG-1000 was added in the solution at a mass ratio to $ZnCl_2$ of 1.5 wt %, and then poured into a three-necked flask. After stirring 0.5 h, a mixed precipitation agents of NaOH and Na_2CO_3 with the molar ratio of n(NaOH): $n(Na_2CO_3) = 2:1$ was added to the flask drop by drop at 60°C with stirring until pH reached about 7.2. After precipitation 2.5 h, the precipitates were filtered and washed three times with distilled water and ethanol, respectively. Finally, the precipitates were dried at 100°C for approximately 12 h in an electric oven to obtain the dried precursor powders.

Preparation of AZO Powders

Figure 1 shows the schematic diagram of the experimental setup of plasma for the preparation of AZO powders. It is composed

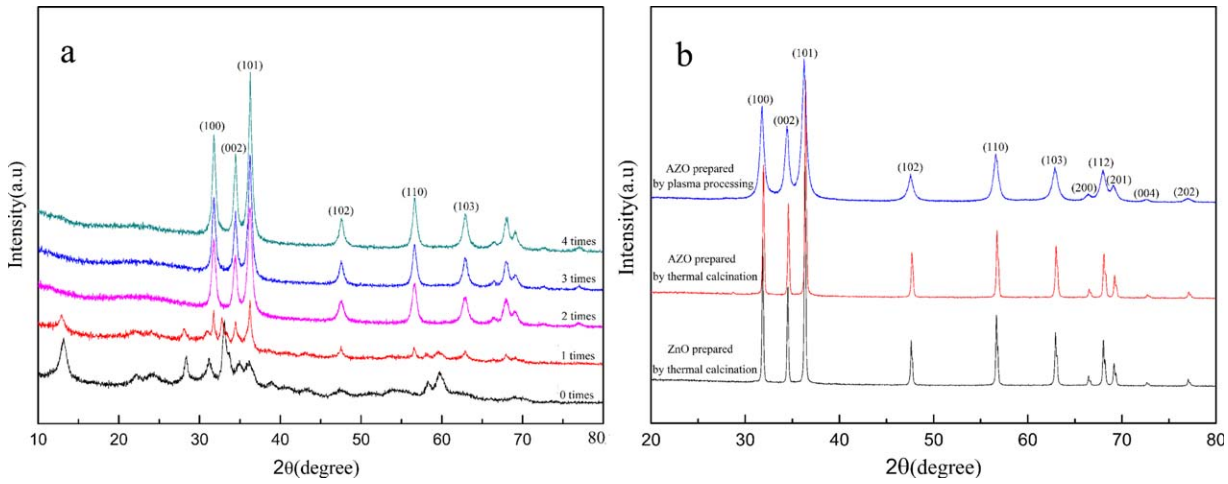

Figure 2. (a) XRD patterns of dried precursor calcined by arc plasma for different times (0, 1, 2, 3, 4.) and (b) XRD patterns of ZnO, AZO powders prepared by thermal calcination at 900°C and AZO powders prepared by plasma processing. [Color figure can be viewed in the online issue, which is available at wileyonlinelibrary.com.]

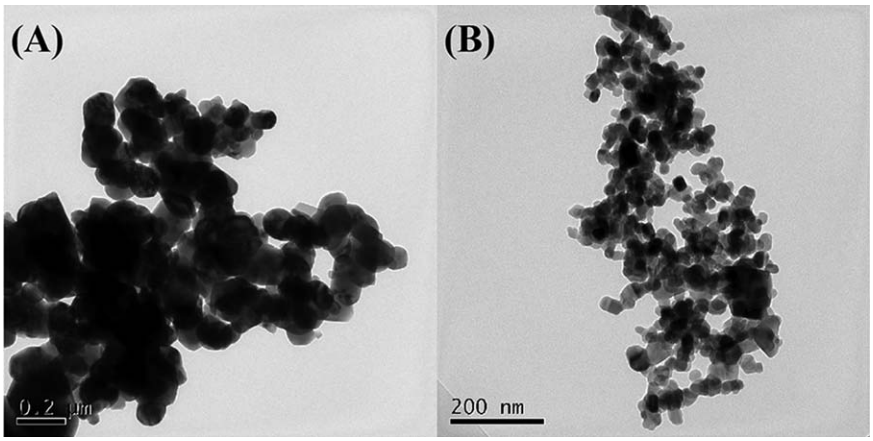

Figure 3. TEM images of AZO powders, (a) Thermal calcination and (b) Plasma processing.

of the arc plasma reactor, the power supply apparatus, the gas feeding pipeline, and the product collecting system. These obtained precursors were treated by arc plasma. First, pure argon was injected to the reaction chamber to remove the air at low flow rate. After 3 min, a certain amount of dried precursors was added to the feed tank and close feed inlet. Then adjust the gas flow rate and an arc discharge was generated at atmospheric pressure. When the argon flow rate increased, the pressure dropped and the drag on individual powders increased. As a result, the powders started to move and be forced to pass through the plasma zone at a fluidization state in the arc plasma reactor. The obtained powders were collected by the sand core funnel, and the operation was repeated five times to ensure that all precursors can be fully treated. The experiments were performed at atmospheric pressure and ambient temperature for the input gases.

For the purpose of comparison, the conventional thermal calcination was used to decompose the dried precursor. To do so, the dried precursor was heated at 900°C for 2 h in an inert argon (Ar) atmosphere with a constant heating rate of 10°C/min.

Preparation of AZO/PP Composites

The AZO powders prepared by plasma were filled into the polypropylene (PP) matrix via a SU-70 B internal mixer (Changzhou Suyan Science and Technology Co., China) at 200°C and 50 rpm for 15 min. The composites were taken out and directly cut into small pellets. To ensure the uniform dispersion, the operation was repeated three times. Then, the pellets were pressed by a plate vulcanizing press at 200°C and 10 MPa for 10 min. For meaningful electrical conductivity measurements and comparison, it is necessary to prepare specimens with consistent shape and size. The obtained composites were cut into rectangles of 10 mm × 3.5 mm × 1.5 mm for electrical conductivity and mechanical properties measurements.

Characterization

The structure of the AZO conductive powders was investigated by X-ray diffraction (XRD) on the Bruker D8ADVANCE X-ray diffractometer at a voltage of 40 kV with Cu Kα radiation ($\lambda = 1.5406$ Å) in the 2θ ranging from 10° to 80°. Transmission electron microscopy (TEM, Hitachi H-600-II, Japan) was conducted at 200 kV to characterize the morphology. For TEM sample preparation, the powders were dispersed in anhydrous ethanol by ultrasonication for 10 min and then fixed on a carbon-coated copper grid (FCF400-Cu). The obtained nanopowders were dispersed in cyclohexane under ultrasonic condition (600 W) with a concentration of 5 mg/mL for UV–Vis analysis. The optical reflect spectra at various concentrations were recorded using an ultraviolet–visible–near infrared (UV–visible–NIR) spectrometer (Varian Cary 50) with a wavelength range of 200–700 nm at room temperature. Thermogravimetric analyzer (TGA Q-50, TA instruments) was used to determine the thermal stability and degradation of pure PP and AZO/PP composites. Approximately 10 mg of the samples were heated at a rate of 20°C/min from room temperature to 800°C under nitrogen atmosphere. The resistivity of the prepared AZO/PP composites was measured by the AC impedance method over a frequency range from 1 Hz to 1 MHz using electrochemical work stations. The average value of each specimen was presented. Tensile strength was determined at room temperature using CMT-6104 testing machine according to GB/T1040-92.

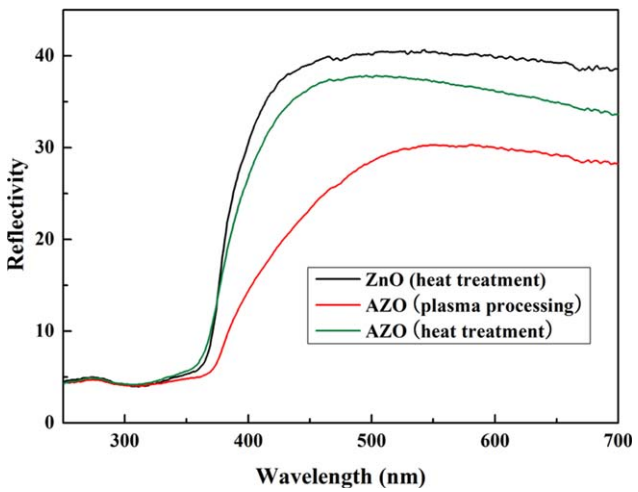

Figure 4. The reflect spectra of ZnO of conventional thermal calcination, AZO of thermal calcination and AZO of plasma processing. [Color figure can be viewed in the online issue, which is available at wileyonlinelibrary.com.]

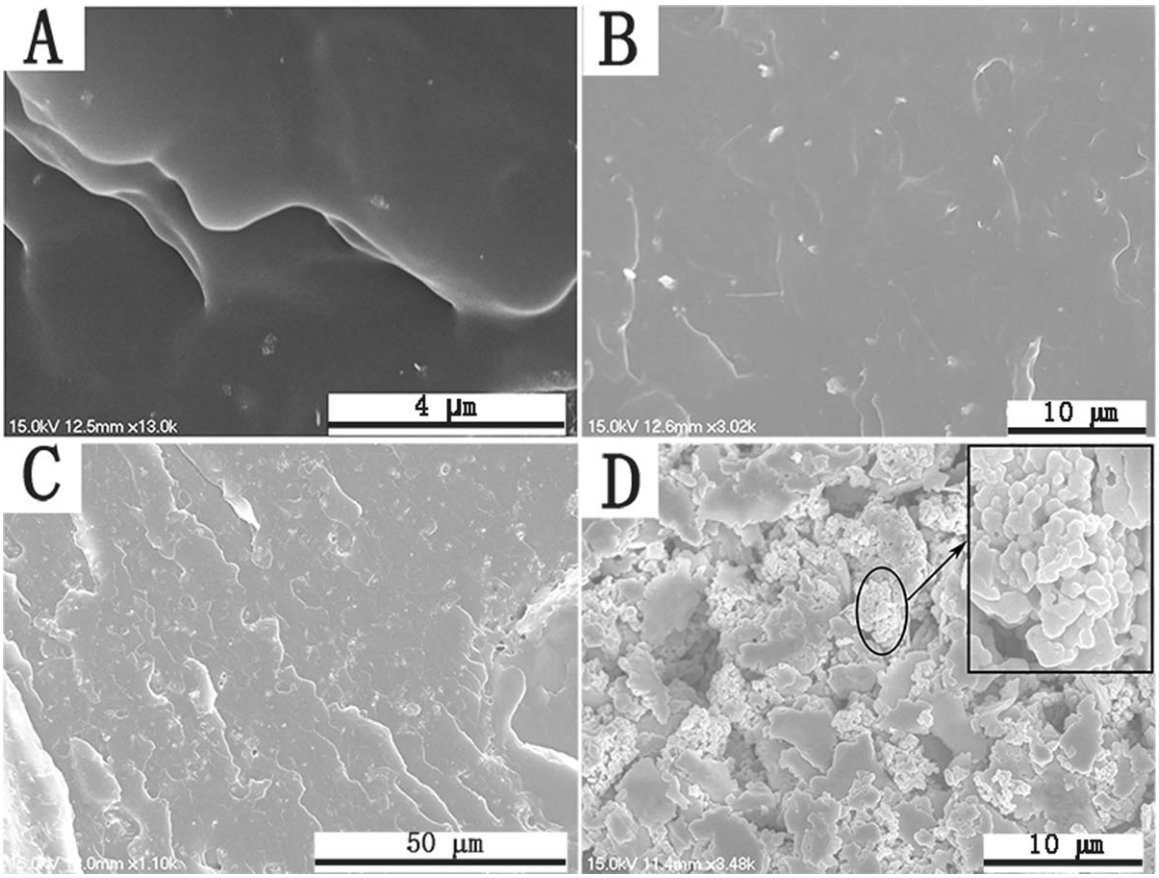

Figure 5. SEM photographs of fracture surfaces for AZO/PP composites: (a) 1 wt %, (b) 3 wt %, (c) 6 wt %, (d) 9 wt %.

Tensile strength was tested at a crosshead speed of 50 mm/min, using dumbbell-shaped specimens with length of 120 mm, gauge length of 30 mm, width of 6 mm, and thickness of 3 mm. Notched IZOD impact test was conducted using XJJ-50machine according to GB/T1043-93.

RESULTS AND DISCUSSION

Structure Property

Figure 2(a) shows the X-ray diffraction patterns of dried precursor calcined by arc plasma for different times (0, 1, 2, 3, 4.). After calcination two times, all diffraction peaks are in good agreement with the typical hexagonal wurtzite structure of ZnO (JCPDS card No. 36–1451). It is evident from the XRD data that there are no extra peaks caused by aluminum metal, other oxides or any zinc aluminum phase, which indicate that the as-synthesized samples are single phase. The Al ion was understood as having substituted the Zn site without changing the wurtzite structure. In addition, with the increase of the processing times the intensity of the characteristic peak gradually strengthened, suggesting that better crystallization can be obtained. The powder XRD patterns of ZnO, AZO powders prepared by conventional thermal calcination at 900°C and AZO powders prepared by plasma processing are shown in Figure 2(b), respectively. It can be seen that all the diffraction peaks are well-matched with those of the hexagonal wurtzite ZnO structure.

Morphological Analysis

The size and morphology of nanoparticles were determined by a transmission electron microscope (TEM) images. The TEM images of the AZO powders of thermal calcination (A) and plasma processing (B) are shown in Figure 3, respectively. It can be seen that all of the AZO nanoparticles of arc plasma processing are hexagonal with a mean size of 30–45 nm, and there is a slight aggregation among the particles. However, the AZO nanoparticles of conventional thermal calcination have aggregated seriously. The results indicated that the plasma technology could effectively reduce the agglomeration among particles. This kind of phenomena may be attributed to the rapid temperatures rise and short sintering time of plasma processing. These advantages made it possible to sinter nanometric powders to approach theoretical values with little grain growth.[36]

Optical Property

Figure 4 shows reflection spectra versus wavelength for the ZnO, AZO of heat treatment, and plasma processing, respectively. In the powder reflection spectra, low reflectance values indicate high absorption in the corresponding wavelength region.[37] From the reflectance curves, we can find that all of the

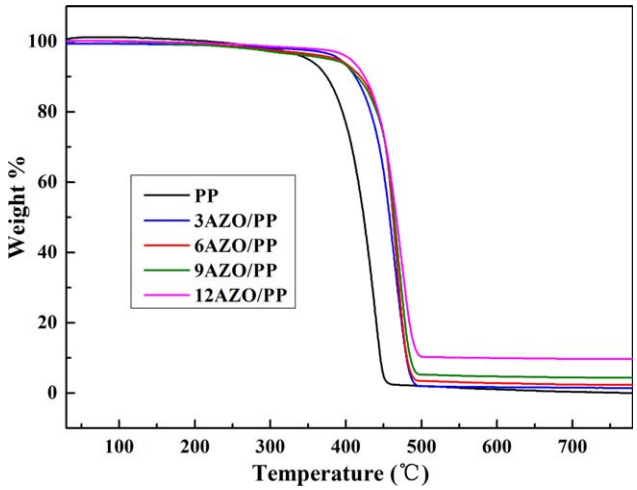

Figure 6. The TGA curve of pure PP and AZO/PP nanocomposites with different content. [Color figure can be viewed in the online issue, which is available at wileyonlinelibrary.com.]

samples have low reflectivity in the UV region, indicating that the samples have excellent absorption of ultraviolet. However, there is an obvious difference between ZnO and AZO nanoparticles. The average reflectance of the ZnO, AZO of heat treatment, and plasma processing are 40, 35, and 27% in the visible range (400–700 nm), respectively. The reflectance of the AZO nanoparticles of plasma processing shows a slight decrease compared with other wavelengths in the VIS region. It possibly related to the gray white coloration present in aluminum-doped zinc oxide produced by this process.

SEM Photographs of Fracture Surfaces for AZO/PP Composites

In this study, the fracture surfaces of the nanocomposites with different filler contents were further examined using scanning electrical micrographs (SEM). Details of the nanocomposite images taken at 1, 3, 6, and 9 wt % AZO content are given in Figure 5(a–d). As can be seen from the photographs, there are few white and gray particles in polypropylene (PP) polymer matrix when the content is 1 wt %, which indicate that highly dense networks could not from in polypropylene (PP) polymer matrix effectively at low content. The nanocomposites containing 3 and 6 wt % AZO show excellent dispersion stability, and the fracture surface of 3 wt % AZO shows smoother, less tearing, and deformation lines. In the nanocomposite of 6 wt % AZO content, we notice a more uniform distribution of the particles with a little quantity of aggregates. For the content of 9 wt %, we can see an aggregate in which we observe a large amount of AZO self-organized in group. The dispersion degree of filler in polymer matrix is related to the filler content.[38,39]

Thermal Stability of AZO/PP Composites

Generally speaking, the polymers are subjected to degradation of the physical and mechanical properties with the increase of temperature. To study the thermal stability of the composites, the TG curves of pure PP and AZO/PP nanocomposite with different concentrations of AZO are shown in Figure 6. The obtained results indicated that the AZO/PP nanocomposites showed better thermal stability than that of the pure PP. The onset of mass loss of pure PP is at about 350°C, and above this temperature, the pure PP decomposes sharply, although the degradation of all the nanocomposites does not emerge at around 350°C. This unique decomposition behavior could be attributed to the presence of AZO in PP. Because of the good interactions between the PP matrix and the powder, the segmental movement of the PP chains was limited. Moreover, the presence of nanoparticles also restrains thermooxidative degradation of the PP at low temperature and the decomposition of hydroperoxides determines the degradation of PP at early stages.[40] Thus, the onset of mass loss of AZO/PP nanocomposites is shifted toward higher temperature.

Mechanical Properties of AZO/PP Composites

The most attractive point for polymer nanocomposite is the enhancement of their mechanical properties and the mechanical parameters are listed in Table I The tensile and notched Izod impact strength of AZO/PP nanocomposites increase with the increasing AZO content in a certain range. This indicates that the dispersion and distribution degree of the AZO in PP are good and the particle could withstand external load during tensile and impact loading, and it fits what the SEM shown. It reaches the maximum tensile strength at 6 wt % AZO content and then decreases. This may be because the non-uniform distribution and agglomeration of AZO nanoparticles in PP matrix cause premature failure. This result is in agreement with the report by Hwang, S. S.[41]

Electrical Properties of AZO/PP Composites

The effects of AZO filler contents on the electrical conductivities of PP were investigated. The result is shown in Figure 7. The results of the electrical conductivity measurements show the expected trend of an increase in conductivity with an increase in filler contents. The conductivity of nanocomposite increases sharply between 0 and 3 wt % AZO loading, indicating the formation of an interconnected structure of AZO and it can be regarded as an electrical percolation. The electrical percolation threshold of the AZO/PP nanocomposite appears at

Table I. Mechanical Properties of the AZO/PP Nanocomposites Filled with Different AZO Content

Filler contents (wt %)	0	3	6	9	12	15
Maximum stress (N)	749.84	892.536	1167.135	1041.071	898.021	536.548
Tensile strength (MPa)	18.74	22.31	29.18	26.03	22.45	13.41
Elastic ratio (N/mm)	337.618	443.543	142.580	232.570	375.795	249.625
Impact strength (KJ/m^2)	25.97	14.37	18.56	18.06	15.24	14.35

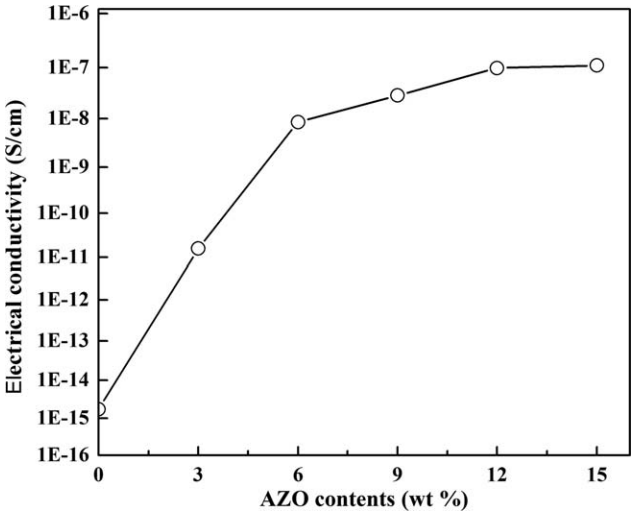

Figure 7. The electrical conductivity of AZO/PP nanocomposites as a function of AZO content.

below 3 wt %, and the nanocomposite occurs a transition from electrical insulator to conductor. When adding 12 wt % AZO, the conductivity is improved by an order of magnitude compared to that of nanocomposite with adding 3 wt % AZO. At 15 wt %, a definite reduction in conductivity is observed, which results from the aggregation and uneven distribution phenomenon of the filler in the PP matrix. The results of the study suggest that it is disadvantageous to use high AZO contents to improve the electrical conductivity of nanocomposites. The conductivity of nanocomposite depends upon the interaction of the AZO filler and matrix, including the dispersion and distribution of the filler in the matrix.

CONCLUSIONS

In conclusion, aluminum-doped ZnO powders have been synthesized by chemical coprecipitation and arc plasma pyrolysis. The excellent properties and application of the as-prepared AZO are summarized as follows:

1. Synthesis method: The facile, economic, and environmentally friendly method implemented for the synthesis of AZO precursor using inexpensive materials is highly favorable and then the precursor was treated by arc plasma. Compared with conventional thermal calcination, arc plasma processing has the advantages of short sintering time, rapid temperature rise and uniform heating for sintered bodies, and marked comparative improvements in properties of optical transmissivity.
2. Excellent properties: the AZO conforms to the hexagonal wurtzite structure of ZnO and possesses high optical transmissivity, low resistivity and good dispersity.
3. Application in PP: the AZO powder with superior physical properties was used as filler in PP matrix. The result showed the proper filling concentration (3 wt %) could form effective and continuous conductive networks within the PP matrix. Furthermore, the obtained nanocomposites possessed higher thermal stability than neat PP. The tensile strength of the AZO/PP nanocomposite is improved significantly by the addition of AZO nanoparticles, and the optimal ZnO content is 6.0 wt %.

ACKNOWLEDGMENTS

The project was supported by the National Natural Science Foundation of China (NNSFC, Nos. 21246002), the National Basic Research Program of China (973 Program, No. 2009CB219904), National Post-doctoral Science Foundation (No. 20090451176), the Jiangsu Provincial Key Lab. of Environmental Materials and Engineering at Yangzhou University (No. K11025), Technology Innovation Foundation of MOST (No. 11C26223204581), Natural Science Foundation of Jiangsu Prov. (No. BK2011328), 333 Talent project (2013) of Jiangsu Prov., the Priority Academic Program Development of Jiangsu Higher Education Institutions (PAPD), and Minjiang Scholarship of Fujian Prov.

REFERENCES

1. Hong, J. I.; Winberg, P.; Schadler, L. S.; Siegel, R. W. *Mater. Lett.* **2005**, *59*, 473.
2. Ye, L.; Meng, X. Y.; Ji, X.; Li, Z. M.; Tang, J. H. *Polym. Degrad. Stab.* **2009**, *94*, 971.
3. Kanmani, P.; Rhim, J. W. *Prog. Nanomater. Food Packaging* **2014**, *35*, 86.
4. Ramasubramaniam, R.; Chen, J.; Liu, H. *Appl. Phys. Lett.* **2003**, *83*, 2928.
5. Shehata, A. B. *Polym. Degrad. Stab.* **2004**, *85*, 577.
6. Taipalus, R.; Harmia, T.; Zhang, M. Q.; Friedrich, K. *Compos. Sci. Technol.* **2001**, *61*, 801.
7. Jiang, J.; Li, G.; Ding, Q.; Mai, K. *Polym. Degrad. Stab.* **2012**, *97*, 833.
8. Yesil, S.; Bayram, G. *J. Appl. Polym. Sci.* **2013**, *127*, 982.
9. Ayrilmis, N.; Kaymakci, A.; Ozdemir, F. *J. Ind. Eng. Chem.* **2013**, *19*, 908.
10. Li, J. H.; Hong, R. Y.; Li, M. Y.; Li, H. Z.; Zheng, Y. *J. Prog. Org. Coating* **2009**, *64*, 504.
11. Zhao, H.; Li, R. K. Y. *Polymer* **2006**, *47*, 3207.
12. Nielsen, L. E. *J. Appl. Polym. Sci.* **1973**, *17*, 3819.
13. Agari, Y.; Uno, T. *J. Appl. Polym. Sci.* **1985**, *30*, 2225.
14. Kalaitzidou, K.; Fukushima, H.; Drzal, L. T. *Carbon* **2007**, *45*, 1446.
15. Elli, T. S.; Dangelo, J. S. *J. Appl. Polym. Sci.* **2003**, *90*, 1639.
16. Wang, Z. L. *Appl. Phys. A- Mater. Sci. Process.* **2007**, *88*, 7.
17. Pawar, B. N.; Cai, G.; Ham, D.; Mane, R. S.; Ganesh, T.; Ghule, A.; Sharmaa, R.; Jadhavab, K. D.; Han, S. H. *Sol. Energ. Mater. Sol. Cell* **2009**, *93*, 524.
18. Ahmad, M.; Ahmed, E.; Zhang, Y.; Khalid, N. R.; Xu, J.; Ullah, M.; Hong, Z. *Curr. Appl. Phys.* **2013**, *13*, 697.
19. Trenque, I.; Mornet, S.; Duguet, E.; Gaudon, M. *Mater. Res. Bull.* **2013**, *48*, 1155.
20. Mahmood, K.; Park, S. B.; Sung, H. J. *J. Mater. Chem. C* **2013**, *1*, 3138.

21. Kim, H.; Osofsky, M.; Prokes, S. M.; Glembocki, O. J.; Piqué, A. *Appl. Phys. Lett.* **2013**, *102*, 171103.
22. Lupan, O.; Chow, L.; Ono, L. K.; Cuenya, B. R.; Chai, G.; Khallaf, H.; Park, S.; Schulte, A. *J. Phys. Chem.* **2010**, *114*, 12401.
23. Kim, Y. S.; Tai, W. P. *Appl. Surf. Sci.* **2007**, *253*, 4911.
24. Jin, M.; Feng, J.; De-Heng, Z.; Hong-lei, M.; Shu-Ying, L. *Thin Solid Films* **1999**, *357*, 98.
25. Kim, D.; Yun, I.; Kim, H. *Curr. Appl. Phys.* **2010**, *10*, S459.
26. Agura, H.; Suzuki, A.; Matsushita, T.; Aoki, T.; Okuda, M. *Thin Solid Films* **2003**, *445*, 263.
27. Yang, W.; Liu, Z.; Peng, D. L.; Zhang, F.; Huang, H.; Xie, Y.; Wu, Z. *Appl. Surf. Sci.* **2009**, *255*, 5669.
28. Wang, Y.; Luo, F.; Zhang, L.; Zhu, D.; Zhou, W. *Cerad. Int.* **2013**, *39*, 8723.
29. Zhang, P.; Hong, R. Y.; Chen, Q.; Feng, W. G. *Powder. Technol.* **2014**, *253*, 360.
30. Lin, Y.; Tang, Z.; Zhang, Z.; Yuan, F.; Ling, Y.; Lee, J.; Huang, S. *J. Am. Ceram. Soc.* **2000**, *83*, 2869.
31. Liu, X. Y.; Hong, R. Y.; Feng, W. G.; Badami, D. *Powder Technol.* **2014**, *256*, 158.
32. Watanabe, T.; Itoh, H.; Ishii, Y. *Thin Solid Films* **2001**, *390*, 44.
33. Farbod, M.; Shoushtari, M. Z.; Parhoodeh, S. *Phys. B: Condens. Matter.* **2011**, *406*, 205.
34. Girshick, S. L.; Chiu, C. P.; Muno, R.; Wu, C. Y.; Yang, L.; Singh, S. K.; McMurry, P. H. *J. Aerosol Sci.* **1993**, *24*, 367.
35. Buchner, P.; Schubert, H.; Uhlenbusch, J.; Willée, K. *Plasma Chem. Plasma Process.* **1999**, *19*, 341.
36. Anselmi-Tamburini, U.; Garay, J. E.; Munir, Z. A.; Tacca, A.; Maglia, F.; Spinolo, G. *J. Mater. Res.* **2004**, *19*, 3255.
37. Yuan, F.; Hu, P.; Yin, C.; Huang, S.; Li, J. *J. Mater. Chem.* **2003**, *13*, 634.
38. Kango, S.; Kalia, S.; Celli, A.; Njuguna, J.; Habibi, Y.; Kumar, R. *Prog. Polym. Sci.* **2013**, *38*, 1232.
39. Seo, M. K.; Lee, J. R.; Park, S. J. *Mater. Sci. Eng A* **2005**, *404*, 79.
40. Razumovskii, L. P.; Gol'dberg, V. M.; Zaikov, G. E. *Polym. Degrad. Stab.* **1994**, *45*, 47.
41. Hwang, S. S.; Hsu, P. P. *J. Ind. Eng. Chem.* **2013**, *19*, 1377.